

Article

Experimental and Numerical Studies on Self-Propagating High-Temperature Synthesis of Ta₅Si₃ Intermetallics

Chun-Liang Yeh *, Chi-Chian Chou and Po-Wen Hwang

Department of Aerospace and Systems Engineering, Feng Chia University, Taichung 40724, Taiwan; E-Mails: rita511235@gmail.com (C.-C.C.); pwhwang@fcu.edu.tw (P.-W.H.)

* Author to whom correspondence should be addressed; E-Mail: clyeh@fcu.edu.tw; Tel.: +886-4-2451-7250 (ext. 3963); Fax: +886-4-2451-0862.

Academic Editor: Ana Sofia Ramos

Received: 11 August 2015 / Accepted: 28 August 2015 / Published: 1 September 2015

Abstract: Formation of Ta₅Si₃ by self-propagating high-temperature synthesis (SHS) from elemental powder compacts of Ta:Si = 5:3 was experimentally and numerically studied. Experimental evidence showed that the increase of either sample density or preheating temperature led to the increase of combustion wave velocity and reaction temperature. The apparent activation energy, $E_a \approx 108$ kJ/mol, was determined for the synthesis reaction. Based upon numerical simulation, the Arrhenius factor of the rate function, $K_0 = 2.5 \times 10^7$ s⁻¹, was obtained for the 5Ta + 3Si combustion system. In addition, the influence of sample density on combustion wave kinetics was correlated with the effective thermal conductivity (k_{eff}) of the powder compact. By adopting $0.005 \leq k_{\text{eff}}/k_{\text{bulk}} \leq 0.016$ in the computation model, the calculated combustion velocity and temperature were in good agreement with experimental data of the samples with compaction densities between 35% and 45% theoretical maximum density (TMD).

Keywords: self-propagating high-temperature synthesis; Ta₅Si₃; numerical simulation; activation energy; Arrhenius factor; thermal conductivity

1. Introduction

Transition metal silicides are of great interest as high-temperature materials, due to their specific properties such as high melting point, good thermal stability, excellent oxidation resistance, good creep

tolerance, and high mechanical strength at elevated temperatures [1–3]. Intermetallic silicides of the Mo–Si, Cr–Si, Ti–Si, V–Si, Nb–Si, and Ta–Si systems are potential candidates for high-temperature applications. In particular, the compounds of the Ta–Si system are among the most refractory silicides with melting points in the range of 2200 to 2500 °C [4]. Preparation of transition metal silicides has been conducted by a variety of fabrication routes, often combining two or more of them, like hot pressing, hot isostatic pressing, reactive sintering, combustion synthesis, mechanical alloying, thermal or plasma spraying, and vapor infiltration [5]. Combustion synthesis in the mode of self-propagating high-temperature synthesis (SHS) is one of the emerging cost-effective techniques and is merited by high energy effectiveness, fast reaction rates, and simple facilities. The SHS method has been applied for the preparation of many advanced materials, including borides, carbides, nitrides, carbonitrides, aluminides, silicides, and complex oxides [6–8].

By means of the classical SHS approach, many silicide phases in the Mo–Si, Ti–Si, Zr–Si, and Nb–Si systems were prepared from the reactant compacts made up of stoichiometric elemental powders [9–12]. In addition, formation of the silicides in the V–Si and Ta–Si systems was carried out by a modified SHS technique known as field-activated combustion synthesis (FACS) that applied an electric field perpendicularly to the propagation direction of the combustion wave [13,14]. Another modification called mechanically-activated SHS (MASHS), which pretreated the reactant powders by prolonged high-energy ball milling at a given frequency and impact energy, was utilized to produce MoSi_2 , TaSi_2 , and Ta_5Si_3 [15,16]. However, despite many studies devoted to the synthesis of intermetallic silicides, the fundamental aspects of reaction rate kinetics and heat transfer parameters on combustion synthesis of metal silicides are scarcely investigated. For the Arrhenius factor (K_0) of the rate function, Li [17,18] adopted $K_0 = 4 \times 10^{10} \text{ s}^{-1}$ to calculate the flame propagation rate of the $\text{Ti} + 2\text{B}$ combustion system. Yeh *et al.* [19] considered the particle size effect and suggested $K_0 = 3 \times 10^8 - 2 \times 10^9 \text{ s}^{-1}$ and $1.5 \times 10^8 - 4 \times 10^8 \text{ s}^{-1}$ for SHS formation of NiAl and CoAl, respectively, from elemental powder compacts. On account of the porous nature of the powder compact, Gennari *et al.* [20,21] introduced an effective thermal conductivity (k_{eff}) equal to 1/70 of the bulk value (k_{bulk}) to their computation model for the study of the SHS process on the formation of transition metal aluminides. Based upon good agreement between measured and calculated combustion wave velocities and temperatures, Yeh *et al.* [19] further indicated that k_{eff} of the Ni–Al powder compacts with relative densities of 50%–65% falls within the extent of $k_{\text{eff}}/k_{\text{bulk}} = 0.016\text{--}0.052$.

The objective of this study is to perform a thorough investigation on combustion synthesis of Ta_5Si_3 from elemental powder compacts of Ta:Si = 5:3. In the experimental part, the effects of sample density and preheating temperature were studied on the combustion wave velocity, reaction temperature, and product composition. The apparent activation energy associated with SHS formation of Ta_5Si_3 was deduced. In the numerical part, the Arrhenius factor of the rate function for the $5\text{Ta} + 3\text{Si}$ combustion system was determined. The effective thermal conductivity of the powder compact was evaluated and correlated with sample density.

2. Experimental and Numerical Methods

For the experiments, tantalum (Aldrich Chemical, <45 μm , 99.9%, St. Louis, MO, USA) and silicon (Strem Chemicals, <45 μm , 99.5%, Newburyport, MA, USA) powders at an atomic ratio of Ta:Si = 5:3

were dry mixed in a ball mill. The reactant mixture was then cold-pressed into cylindrical compacts with a diameter of 7 mm and a height of 12 mm. The sample density (d_s) of the powder compact was a studied variable, which considered three values in terms of 35%, 40%, and 45% of the theoretical maximum density (TMD). In a stainless-steel windowed chamber under high-purity argon (99.99%), the experiment was performed with samples at different preheating temperatures (T_p) from room temperature (25 °C) to 300 °C. This study measured the combustion wave velocity and reaction temperature, and identified the phase constituents of SHS-derived products. Details of the experimental setup were reported elsewhere [22]. In addition, the apparent activation energy (E_a) of the synthesis reaction was determined from the dependence of combustion wave velocity on the reaction temperature [10,11].

In the simulation model, an energy equation expressed as Equation (1) was numerically solved to obtain the transient sample temperature profile during the propagation of a self-sustaining combustion wave [19].

$$\rho C_p \frac{\partial T}{\partial t} = k_{\text{eff}} \frac{\partial^2 T}{\partial x^2} + \rho Q \phi(T, \eta) - \frac{4h(T - T_0)}{d} - \frac{4\sigma\varepsilon(T^4 - T_0^4)}{d} \quad (1)$$

where C_p is the heat capacity of the product, k_{eff} the effective thermal conductivity, Q the exothermic heat of the reaction, $\phi(T, \eta)$ the reaction rate function, h the convection heat transfer coefficient, σ the Stefan-Boltzmann constant, ε the emissivity, and d the diameter of the test specimen. The rate function of $\phi(T, \eta)$ is given by an Arrhenius form (Equation (2)) [18,19].

$$\phi(T, \eta) = \frac{\partial \eta}{\partial t} = K_0(1 - \eta) \exp\left(-\frac{E_a}{RT}\right) \quad (2)$$

where η is the fraction of the reactant transformed into the product, K_0 the Arrhenius factor, and E_a the activation energy. The numerical scheme as well as the initial and boundary conditions were previously described [19]. The effective thermal conductivity of Equation (1) is essentially affected by the porosity of the test specimen. To account for the significant variation of k_{eff} with sample density [19,23], the ratio of $k_{\text{eff}}/k_{\text{bulk}}$ between 0.002 and 0.05 was considered in the numerical model of this study.

3. Results and Discussion

3.1. Experimental Measurement and Analysis

A typical sequence of combustion images recorded from a powder compact of Ta:Si = 5:3 is illustrated in Figure 1, showing that a steady and nearly parallel combustion wave traveling in a self-sustaining fashion. Based upon the recorded films, the deduced flame-front propagation velocity (V_f) varying from 6.4 to 22.9 mm/s was reported in Figure 2 as a function of sample density and preheating temperature. As the sample density increased from 35% to 45% TMD, an appreciable increase in the flame-front velocity was observed. This was primarily caused by the enhancement of intimate contact between the reactant particles, which improved the layer-by-layer heat transfer and accelerated the combustion wave. In addition, owing to the increase of the reaction temperature with initial sample temperature, Figure 2 shows that the propagation rate of the combustion wave increases

considerably with sample preheating temperature. It is useful to note that an increase in T_p from 25 to 300 °C almost doubles the flame-front velocity.

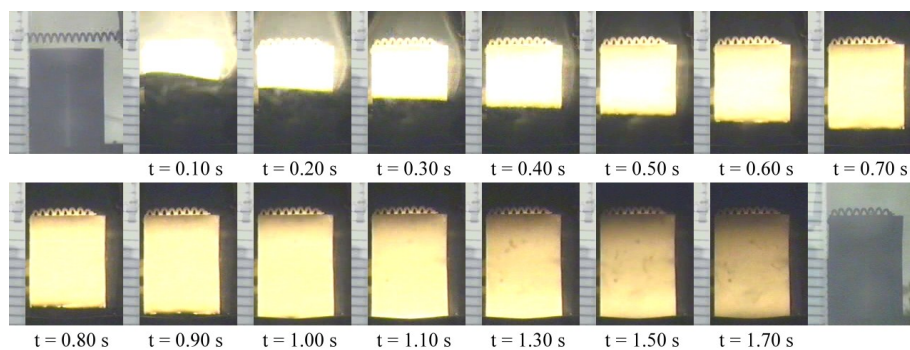


Figure 1. Solid state combustion propagating in a self-sustaining manner along a powder compact of Ta:Si = 5:3 with $d_s = 35\%$ TMD and $T_p = 100$ °C.

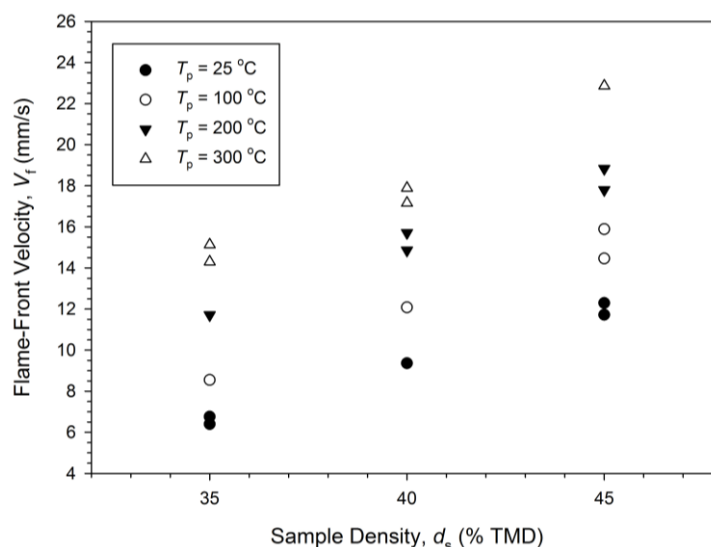


Figure 2. Effects of sample density and preheating temperature on flame-front velocity of elemental powder compacts of Ta:Si = 5:3.

The dependence of the combustion front temperature (T_c) on sample density and preheating temperature is presented in Figure 3. According to the typical temperature profiles plotted in the insert of Figure 3, the abrupt rise in the temperature represents rapid arrival of the reaction front and the peak value signifies the combustion front temperature. Data points in Figure 3 signify the combustion front temperatures. In the insert, two temperature profiles measured from 45% TMD samples with $T_p = 100$ and 300 °C are presented. It is evident that the increase of preheating temperature increases the reaction temperature. As shown in Figure 3, for the samples without prior heating ($T_p = 25$ °C), the increase of sample density from 35% to 45% TMD significantly increased the peak combustion temperature from 1240 to 1530 °C. This could be attributed to a lesser amount of heat dissipated within the voids of the porous compact. As a result, the energy flux sustaining the combustion wave propagation was augmented. The combustion front temperature was also increased by preheating the sample. It was found that a more substantial increase of the combustion front temperature by

preheating the sample was observed for the sample with a lower compaction density. Likewise, the influence of sample density was more pronounced for the sample with a lower preheating temperature. The highest combustion temperature reaching up to 1645 °C was measured from the sample of 45% TMD at $T_p = 300$ °C.

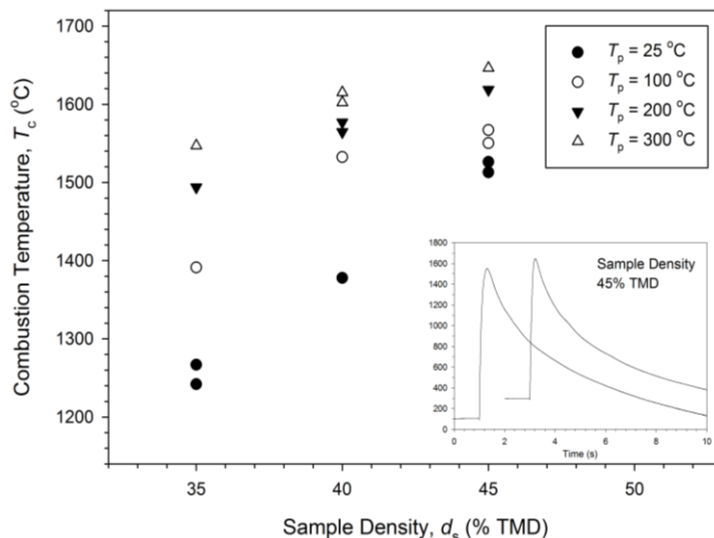


Figure 3. Effects of sample density and preheating temperature on combustion temperature of elemental powder compacts of Ta:Si = 5:3.

In order to determine the apparent activation energy (E_a) of the self-sustaining combustion reaction associated with formation of Ta_5Si_3 , the following equation that relates the combustion wave velocity with the combustion temperature and the thermochemical parameters is considered [10,11].

$$\left(\frac{V_f}{T_c}\right)^2 = f(n)K\left(\frac{R}{E_a}\right)\exp\left(-\frac{E_a}{RT_c}\right) \quad (3)$$

where $f(n)$ is a function of the kinetic order of the reaction, R the universal gas constant, and K a constant which includes the heat capacity of the product, the thermal conductivity, and the heat of the reaction. Based upon Equation (3), a plot correlating $\ln(V_f/T_c)^2$ with $1/T_c$ is constructed in Figure 4. According to the slope of a best-fitted straight line for the data, $E_a \approx 108$ kJ/mol was obtained and employed in the reaction rate function of Equation (2) for the numerical simulation.

Figure 5 presents the XRD patterns of two synthesized products from samples of different densities and preheating temperatures. It is evident that Ta_5Si_3 was formed as the dominant silicide and a minor phase Ta_2Si was identified. A comparison between Figure 5a,b indicates that the content of Ta_2Si was reduced by increasing the sample compaction density and initial temperature. This implies that higher reaction temperature and better contact between the reactant powders could enhance the phase conversion.

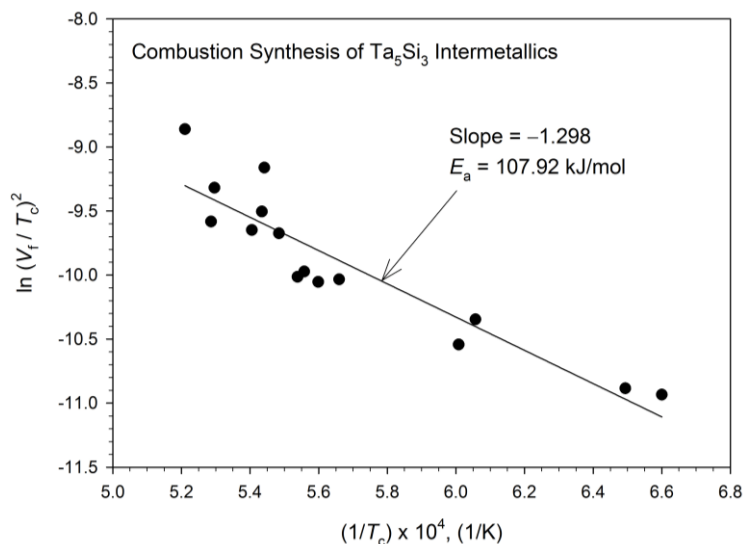


Figure 4. Activation energy (E_a) of combustion synthesis of Ta_5Si_3 determined from a relationship between combustion front velocity (V_f) and temperature (T_c).

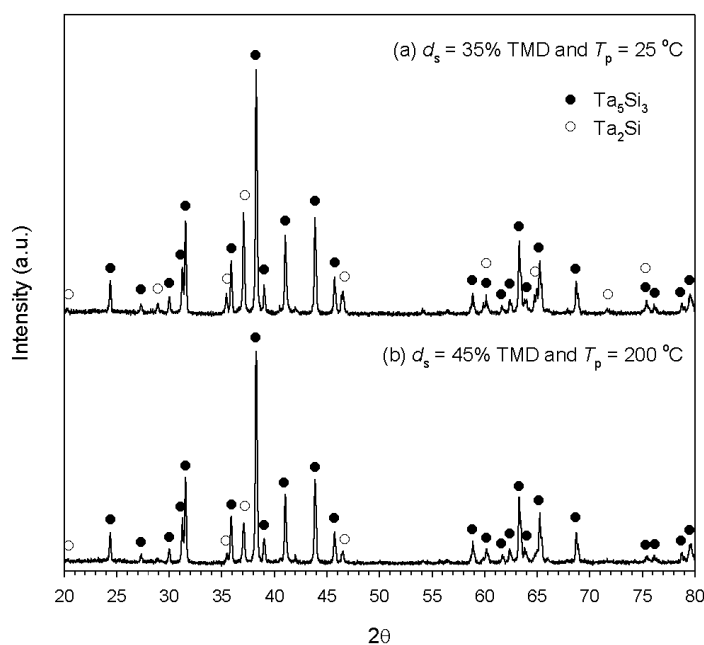


Figure 5. X-ray diffraction (XRD) patterns of SHS-derived products from Ta:Si = 5:3 powder compacts with (a) $d_s = 35\%$ TMD and $T_p = 25\text{ }^\circ\text{C}$ and (b) $d_s = 45\%$ TMD and $T_p = 200\text{ }^\circ\text{C}$.

3.2. Numerical Simulation and Validation

The Arrhenius factor (K_0) of the rate function is essentially dissimilar for different reaction systems. According to the previous study [19], the magnitude of K_0 varies between 1.5×10^8 and $2.0 \times 10^9\text{ s}^{-1}$ for combustion synthesis of intermetallic aluminides, CoAl and NiAl. It should be noted that very high combustion rates were detected in the Co–Al and Ni–Al combustion systems. Specifically, for the powder compacts with no prior heating, the flame-front velocity in the range of 11–37 mm/s was measured for the Co–Al system and 22–102 mm/s for the Ni–Al system [19]. In a series of numerical

simulation performed by this study, the calculated results with $0.005 \leq k_{\text{eff}}/k_{\text{bulk}} \leq 0.02$ and $T_p = 25 \text{ }^\circ\text{C}$ showed that the adoption of $K_0 = 3.0 \times 10^9 \text{ s}^{-1}$ in the model yields $V_f = 18\text{--}32 \text{ mm/s}$, $K_0 = 3.0 \times 10^8 \text{ s}^{-1}$ yields $V_f = 12\text{--}20 \text{ mm/s}$, $K_0 = 3.0 \times 10^7 \text{ s}^{-1}$ yields $V_f = 8\text{--}12 \text{ mm/s}$, and $K_0 = 3.0 \times 10^6 \text{ s}^{-1}$ yields $V_f = 4\text{--}8 \text{ mm/s}$. The above results advised that the magnitude of K_0 on the order of 10^7 is the best fit for the Ta–Si combustion system. After a further refinement coupled with appropriate values of $k_{\text{eff}}/k_{\text{bulk}}$, it was found that $K_0 = 2.5 \times 10^7 \text{ s}^{-1}$ is the optimum to achieve the most agreeable results between measured and calculated combustion wave velocities for the 5Ta + 3Si combustion system.

Figure 6a,b plots the calculated instantaneous temperature profiles during the SHS process for the 5Ta + 3Si powder compacts with different effective thermal conductivities and preheating temperatures. The test specimen with a ratio of $k_{\text{eff}}/k_{\text{bulk}} = 1.0$ signifies a fully-dense sample, while that with $0 < k_{\text{eff}}/k_{\text{bulk}} < 1$ represents the powder compact with a certain degree of porosity. As depicted in Figure 6a, for the case of $k_{\text{eff}}/k_{\text{bulk}} = 0.005$ and $T_p = 25 \text{ }^\circ\text{C}$, the combustion wave at $t = 1.8 \text{ s}$ is about to reach the bottom of the sample and the deduced flame-front velocity was 6.59 mm/s . Figure 6a also reveals the profiles featuring a comparable peak temperature of around $1260 \text{ }^\circ\text{C}$, which stands for the combustion front temperature. For the powder compact with $k_{\text{eff}}/k_{\text{bulk}} = 0.02$ and $T_p = 200 \text{ }^\circ\text{C}$, as shown in Figure 6b, the combustion front temperature rises to $1535 \text{ }^\circ\text{C}$ and the time required to complete the SHS process is noticeably shortened by a faster combustion front with $V_f = 20.22 \text{ mm/s}$. The increase of k_{eff} is to numerically simulate the powder compact with a higher compaction density, which corresponds to the possession of a better degree of contact between the reactant powders. As a result, the rate of heat transfer from the combustion front to the unburned region is enhanced and the heat lost to the voids of the porous sample is reduced. This explains a faster combustion wave and a higher reaction front temperature for a denser powder compact. Preheating the sample also contributes to a higher reaction temperature, which favors the propagation of the combustion front. The calculated combustion velocities and temperatures of Figure 6 are within a reasonable range consistent with the experimental data, which confirms the reaction kinetics and exothermicity of the numerical model.

Figure 7 presents a comparison between measured and calculated flame-front velocities for combustion synthesis of Ta_5Si_3 . The symbols plotted in Figure 7 are experimental data obtained from the 5Ta + 3Si samples and the continuous solid lines represent the computational results under $K_0 = 2.5 \times 10^7 \text{ s}^{-1}$ and $0.005 \leq k_{\text{eff}}/k_{\text{bulk}} \leq 0.016$. It is evident that for different preheating temperatures, the calculated flame speeds agree satisfactorily with experimental data of the samples with densities of 35%–45% TMD. The determination of the ratio of $k_{\text{eff}}/k_{\text{bulk}}$ not only has to yield the calculated combustion velocities in good agreement with experimental data, but should also be consistent with that reported by the previous study [19]. As mentioned above, k_{eff} of the Ni–Al powder compacts with relative densities of 50%–65% TMD falls within the extent of $k_{\text{eff}}/k_{\text{bulk}} = 0.016\text{--}0.052$. Therefore, the magnitudes of $k_{\text{eff}}/k_{\text{bulk}} = 0.005\text{--}0.016$ and $K_0 = 2.5 \times 10^7 \text{ s}^{-1}$ were justified for combustion synthesis of Ta_5Si_3 from elemental powder compacts of 35%–45% TMD.

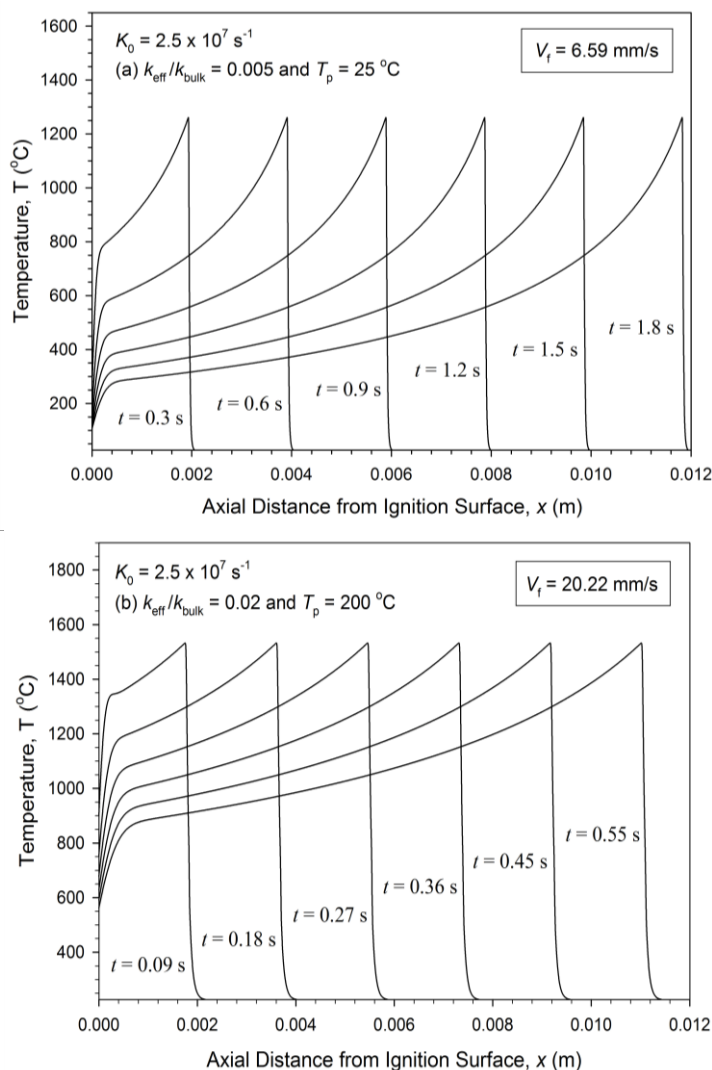


Figure 6. Calculated time histories of temperature profiles of Ta–Si powder compacts with (a) $k_{\text{eff}}/k_{\text{bulk}} = 0.005$ and $T_p = 25 \text{ °C}$ and (b) $k_{\text{eff}}/k_{\text{bulk}} = 0.02$ and $T_p = 200 \text{ °C}$.

4. Conclusions

Formation of Ta_5Si_3 by combustion synthesis in the SHS mode was experimentally and numerically investigated by this study. Sample compacts with $d_s = 35\%$, 40% and 45% TMD were prepared from an elemental powder mixture of Ta:Si = 5:3. Experiments were conducted with powder compacts at different preheating temperatures of $T_p = 25\text{--}300 \text{ °C}$. It was found that both the measured combustion wave velocity ranging from 6.4 to 22.9 mm/s and combustion temperatures from 1240 to 1645 °C increased with increasing sample density and preheating temperature. The apparent activation energy, $E_a \approx 108 \text{ kJ/mol}$, of the synthesis reaction was deduced from the dependence of combustion wave velocity on reaction temperature. Formation of Ta_5Si_3 as the dominant silicide phase from solid-state combustion was achieved. A minor phase Ta_2Si was reduced by increasing the sample density and combustion temperature.

In the numerical study, the Arrhenius factor of the rate function, $K_0 = 2.5 \times 10^7 \text{ s}^{-1}$, was obtained to optimally simulate the combustion rate of the $5\text{Ta} + 3\text{Si}$ sample to form Ta_5Si_3 . The effect of sample density on combustion wave kinetics was correlated with the variation of k_{eff} of the powder compact.

Numerical simulations showed that the calculated combustion velocities and their dependent trend based upon $0.005 \leq k_{\text{eff}}/k_{\text{bulk}} \leq 0.016$ properly matched the experimental data of the samples with 35%–45% TMD. Moreover, the combustion exothermicity of the numerical model was well justified by the measured combustion temperatures.

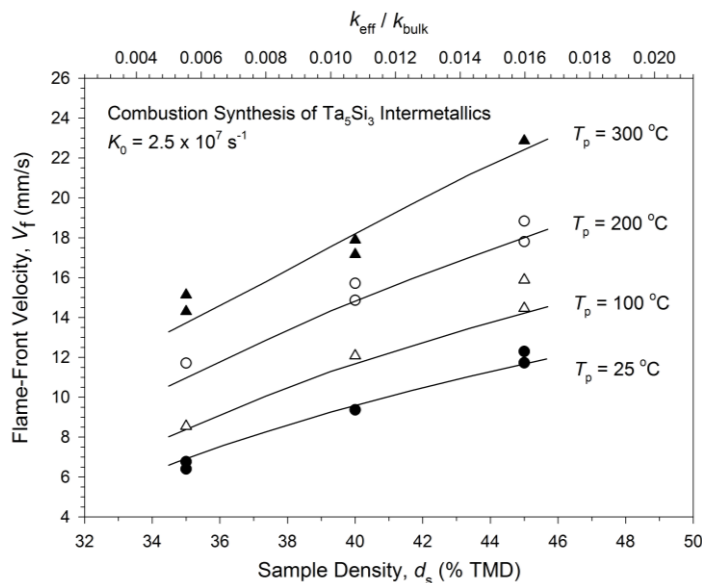


Figure 7. A comparison between measured and calculated flame-front velocities as functions of sample density and $k_{\text{eff}}/k_{\text{bulk}}$ for combustion synthesis of Ta_5Si_3 .

Acknowledgments

This research was sponsored by the Ministry of Science and Technology, ROC under the grant of MOST 104-2221-E-035-057. The authors are grateful for the Precision Instrument Support Center of Feng Chia University in providing materials analytical facilities.

Author Contributions

C.-L. Yeh supervised the work, wrote the paper, and analyzed the experimental and numerical data; C.-C. Chou conducted the experiments and performed numerical simulation; and P.-W. Hwang contributed the numerical modeling.

Conflicts of Interest

The authors declare no conflict of interest.

References

1. Meschter, P.J.; Schwartz, D.S. Silicide-matrix materials for high temperature applications. *JOM* **1989**, *41*, 52–55.
2. Petrovic, J.J.; Vasudevan, A.K. Key developments in high temperature structural silicides. *Mater. Sci. Eng. A* **1999**, *261*, 1–5.

3. Tillard, M. The mixed intermetallic silicide $Nb_{5-x}Ta_xSi_3$ ($0 \leq x \leq 5$). Crystal and electronic structure. *J. Alloy. Compd.* **2014**, *584*, 385–392.
4. Schlesinger, M.E. Thermodynamics of solid transition-metal silicides. *Chem. Rev.* **1990**, *90*, 607–628.
5. Stoloff, N.S. An overview of powder processing of silicides and their composites. *Mater. Sci. Eng. A* **1999**, *261*, 169–180.
6. Liu, G.; Li, J.; Chen, K. Combustion synthesis of refractory and hard materials: A review. *Int. J. Refract. Met. Hard Mater.* **2013**, *39*, 90–102.
7. Gromov, A.A.; Chukhlomina, L.N. *Nitride Ceramics: Combustion Synthesis, Properties, and Applications*; Wiley-VCH: Weinheim, Germany, 2015.
8. Vicario, I.; Poulon-Quintin, A.; Lagos, M.A.; Silvain, J.F. Effect of material and process atmosphere in the preparation of Al–Ti–B grain refiner by SHS. *Metals* **2015**, *5*, 1387–1396.
9. Yeh, C.L.; Chen, W.H. Combustion synthesis of $MoSi_2$ and $MoSi_2$ – Mo_5Si_3 composites. *J. Alloy. Compd.* **2007**, *438*, 165–170.
10. Yeh, C.L.; Chen, W.H.; Hsu, C.C. Formation of titanium silicides Ti_5Si_3 and $TiSi_2$ by self-propagating combustion synthesis. *J. Alloy. Compd.* **2007**, *432*, 90–95.
11. Bertolino, N.; Anselmi-Tamburini, U.; Maglia, F.; Spinolo, G.; Munir, Z.A. Combustion synthesis of Zr–Si intermetallic compounds. *J. Alloy. Compd.* **1999**, *288*, 238–248.
12. Yeh, C.L.; Chen, W.H. Preparation of Nb_5Si_3 intermetallic and Nb_5Si_3/Nb composite by self-propagating high-temperature synthesis. *J. Alloy. Compd.* **2005**, *402*, 118–123.
13. Maglia, F.; Anselmi-Tamburini, U.; Milanese, C.; Bertolino, N.; Munir, Z.A. Field activated combustion synthesis of the silicides of vanadium. *J. Alloy. Compd.* **2001**, *319*, 108–118.
14. Maglia, F.; Anselmi-Tamburini, U.; Bertolino, N.; Milanese, C.; Munir, Z.A. Field-activated combustion synthesis of Ta–Si intermetallic compounds. *J. Mater. Res.* **2001**, *16*, 534–544.
15. Gras, C.; Gaffet, E.; Bernard, F. Combustion wave structure during the $MoSi_2$ synthesis by mechanically-activated self-propagating high-temperature synthesis (MASHS): *In situ* time-resolved investigations. *Intermetallics* **2006**, *14*, 521–529.
16. Maglia, F.; Milanese, C.; Anselmi-Tamburini, U.; Doppiu, S.; Cocco, G.; Munir, Z.A. Combustion synthesis of mechanically activated powders in the Ta–Si system. *J. Alloy. Compd.* **2004**, *385*, 269–275.
17. Li, H.P. The numerical simulation of the heterogeneous composition effect on the combustion synthesis of TiB_2 compound. *Acta Mater.* **2003**, *51*, 3213–3224.
18. Li, H.P. An investigation of the ignition manner effects on combustion synthesis. *Mater. Chem. Phys.* **2003**, *80*, 758–767.
19. Yeh, C.L.; Hwang, P.W.; Chen, W.K.; Li, J.Y. Modeling evaluation of Arrhenius factor and thermal conductivity for combustion synthesis of transition metal aluminides. *Intermetallics* **2013**, *39*, 20–24.
20. Gennari, S.; Maglia, F.; Anselmi-Tamburini, U.; Spinolo, G. SHS (Self-sustained high-temperature synthesis) of intermetallic compounds: Effect of process parameters by computer simulation. *Intermetallics* **2003**, *11*, 1355–1359.

21. Gennari, S.; Anselmi-Tamburini, U.; Maglia, F.; Spinolo, G.; Munir, Z.A. A new approach of the modeling of SHS reactions: Combustion synthesis of transition metal aluminides. *Acta Mater.* **2006**, *54*, 2343–2351.
22. Yeh, C.L.; Lin, J.Z. Combustion synthesis of Cr–Al and Cr–Si intermetallics with Al₂O₃ additions from Cr₂O₃–Al and Cr₂O₃–Al–Si reaction systems. *Intermetallics* **2013**, *33*, 126–133.
23. Miura, S.; Terada, Y.; Suzuki, T.; Liu, C.T.; Mishima, Y. Thermal conductivity of Ni–Al powder compacts for reaction synthesis. *Intermetallics* **2000**, *8*, 151–155.

© 2015 by the authors; licensee MDPI, Basel, Switzerland. This article is an open access article distributed under the terms and conditions of the Creative Commons Attribution license (<http://creativecommons.org/licenses/by/4.0/>).